Published in IET Microwaves, Antennas & Propagation
Received on 28th March 2007
Revised on 12th November 2007
doi: 10.1049/iet-map:20070076

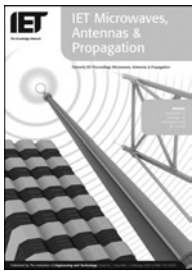

ISSN 1751-8725

Eigenspace-based blind pattern optimisations of steerable antenna array for interference cancellation

S. Sugiura[1] *N. Kikuma*[2] *H. Iizuka*[1]

[1], *Toyota Central Research and Development Laboratories, Inc., Nagakute, Aichi480-1192, Japan*
[2]*Nagoya Institute of Technology, Nagoya, Aichi466-8555, Japan*
E-mail: sugiura@mosk.tytlabs.co.jp

Abstract: A novel adaptive algorithm for an array using directional elements called a hybrid smart antenna system is proposed. The algorithm controls the element patterns on the basis of an objective function composed of eigenvalues of a covariance matrix. A high and stable array output signal-to-interference-plus-noise ratio is achieved by improving both the received powers and the spatial correlation coefficient between incident waves, without prior knowledge such as directions-of-arrival, channel state information or training signals. The characteristics of the proposed algorithm are theoretically and numerically clarified for a simple case involving two incident waves. Convergence with least mean squares algorithm is found to be as fast as that with recursive least squares algorithm in this system. Also, simulation for statistical performance evaluation is carried out in comparison with a conventional system. Furthermore, a method to implement the proposed eigenspace control algorithm without having to solve the eigenvalue problem is shown.

1 Introduction

Recently, there has been a great deal of interest in improving the capacities of telecommunication networks for the rapid increase of users. Space division multiple access (SDMA) using smart antenna systems is one of the promising candidates to realise highly efficient frequency utilisation [1]. So far, several types of smart antenna systems and algorithms have been studied. Many smart antenna systems use adaptive antenna arrays based on digital beamforming (DBF) techniques to control complex variable weights [2]. DBF antenna arrays achieve high performance of interference suppression while receiving a desired signal. However, the main drawbacks of DBF antenna arrays are their high cost and large size, which are caused by multiple RF receivers as many as antenna elements.

To realise a simpler system, some types of analog beamforming (ABF) antennas with a single RF port have been developed. The examples include switched-beam antennas using directional elements [3, 4]. Alternatively, reactively steered antennas have been developed [5–7], which continuously control directivity by changing the reactance values of reactance circuits embedded in the antenna. Adaptive algorithms to control such a reactively steered antenna were also developed [8, 9]. However, ABF antennas are inferior to DBF antenna arrays in quality because of having only one RF port.

To utilise the advantages of both DBF antenna arrays and ABF antennas, hybrid smart antenna systems have been designed and developed [10–12]. The hybrid smart antenna systems are characterised by multiple RF ports with variable element patterns and/or positions, aiming to reduce the number of the RF ports without degrading performance. Two-stage controls are implemented. First, patterns of elements connected to RF ports are determined depending on the predetermined rules. At the second stage, complex weights are determined using traditional algorithms developed in the field of adaptive antennas.

The array output signal-to-interference-plus-noise ratio (SINR) using complex weight control is greatly influenced by the spatial correlation coefficient between the desired

and interference signals [13]. The spatial correlation coefficient is expressed by the array configuration (element positions and patterns) and directions of arrival (DOA). By taking appropriate control of the element patterns depending on the radio wave environment, hybrid smart antenna systems may enable adaptive improvement not only in input power but also in the spatial correlation coefficient. However, direct improvement of the spatial correlation coefficient requires a priori knowledge such as DOA, channel state information (CSI) or training signals. For this reason, a blind algorithm for reducing the spatial correlation coefficient has not been found as far as the authors know. In fact, previous hybrid smart antenna systems control the elements only depending on the input power of each branch [11, 12].

This paper proposes a novel adaptive algorithm to control the directional elements of a hybrid smart antenna system. The algorithm utilises an objective function composed of eigenvalues of a covariance matrix, and enables improvement in both input power and spatial correlation coefficient without prior knowledge. This algorithm is therefore called an eigenspace control algorithm. The present paper is primarily focused on this first-stage control of hybrid smart antenna system, that is, pattern optimisations. This paper is organised as follows. The system configuration, proposed algorithm and theoretical characteristics are described in Section 2. Section 3 contains the results of computer simulation performed to verify the characteristics. Subsequently, the performance of the proposed system in comparison with a conventional system is discussed. Then a method of reducing computational load by modifying the proposed algorithm is also described. Finally, a conclusion is given in Section 4. The mathematical inequalities used in Section 2 are derived in the appendix.

2 Eigenspace control

This section describes the proposed eigenspace control algorithm for optimising directional elements of a hybrid smart antenna system.

2.1 Configuration of hybrid smart antenna system

A configuration of a K-element hybrid smart antenna system is shown in Fig. 1. $f_k(\phi)$ $(k = 1, \ldots, K)$ represents the complex response patterns of the elements at an azimuth angle ϕ. In this system, they are controlled adaptively as well as complex variable weights w_k $(k = 1, \ldots, K)$ which are expressed by a column vector $\boldsymbol{w}$ given by

$$\boldsymbol{w} = \begin{bmatrix} w_1 & w_2 & \cdots & w_K \end{bmatrix}^{\mathrm{T}} \tag{1}$$

where the superscript T denotes the transpose. Likewise, the complex baseband signals s_k $(k = 1, \ldots, K)$ received at all

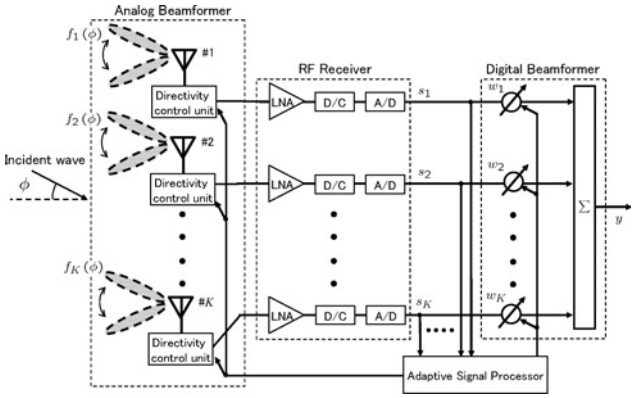

Figure 1 *Configuration of hybrid smart antenna system using K directly-controlled elements*

elements are expressed as follows

$$\boldsymbol{s} = \begin{bmatrix} s_1 & s_2 & \cdots & s_K \end{bmatrix}^{\mathrm{T}} \tag{2}$$

Thus, array output y is given by

$$y = \boldsymbol{w}^{\mathrm{H}}\boldsymbol{s} \tag{3}$$

where the superscript H denotes the complex conjugate transpose.

For the case of two uncorrelated incident waves such as a desired signal at ϕ_d and an interference signal at ϕ_u, the array output SINR using optimum weights is derived as follows [13]

$$\mathrm{SINR} = \frac{P_d \tilde{D}(\phi_d)}{P_n}\left(1 - \frac{P_u \tilde{D}(\phi_u)}{P_n + P_u \tilde{D}(\phi_u)}|\rho|^2\right) \tag{4}$$

where

$$\rho = \frac{\boldsymbol{v}(\phi_d)^{\mathrm{H}}\boldsymbol{v}(\phi_u)}{\|\boldsymbol{v}(\phi_d)\|\|\boldsymbol{v}(\phi_u)\|} \tag{5}$$

is the spatial correlation coefficient bounded by zero and one and

$$\tilde{D}(\phi) = |f_1(\phi)|^2 + |f_2(\phi)|^2 + \cdots + |f_K(\phi)|^2 \tag{6}$$

is the sum over the complex array response patterns resulting from coherent combining. Also, $\boldsymbol{v}(\phi)$ is the combination of the array response vector and antenna pattern, and is given by

$$\boldsymbol{v}(\phi) = \left[f_1(\phi)\ f_2(\phi)\exp\left(-j\frac{2\pi}{\lambda}d\sin\phi\right) \cdots f_K(\phi)\exp\left(-j\frac{2\pi}{\lambda}(K-1)d\sin\phi\right)\right]^{\mathrm{T}} \tag{7}$$

for the uniform linear array with an element spacing of d. P_d and P_u are signal powers of the desired and interference signals, respectively. Each of the signal powers is defined as a value that would be received by an isotropic antenna. P_n

is the thermal noise power of the elements. Consequently, the input signal-to-noise ratio (SNR) and input interference-to-noise ratio (INR) are defined by P_d/P_n and P_u/P_n, respectively. As shown in (4), the array output SINR can be improved by reducing $|\rho|$ and increasing $\tilde{D}(\phi_d)$. However, it should be noted that the desired and interference signals cannot be classified a priori in a practical system.

2.2 Novel algorithm

The proposed algorithm for determining element patterns is implemented by maximising one of the three types of objective functions J_i $(i = 1, 2, 3)$, which are given by

$$J_1 = \lambda_M \tag{8}$$

$$J_2 = \lambda_1 \cdots \lambda_M \tag{9}$$

$$J_3 = \frac{\lambda_1 \cdots \lambda_M}{\lambda_1 + \cdots + \lambda_M} \tag{10}$$

where M is the number of uncorrelated incident waves and λ_i $(i = 1, \ldots, K)$ are eigenvalues of the covariance matrix R given by

$$R = E[\boldsymbol{s}\boldsymbol{s}^{\mathrm{H}}] \tag{11}$$

where $E[\,]$ denotes expectation. Thus, λ_i and R are associated with the equation

$$R\boldsymbol{e}_i = \lambda_i \boldsymbol{e}_i \tag{12}$$

and $\boldsymbol{e}_i$ is the eigenvector corresponding to λ_i. Also, it is assumed that the eigenvalues have the relation

$$\lambda_i \geq \lambda_j \quad (i < j) \tag{13}$$

and that $K \geq M$ throughout this paper. Each of the objective functions is composed of the eigenvalues which belong to the signal subspace of the covariance matrix. The proposed algorithm leads to the maximisation of the total received powers in the signal subspace.

A case with two incident waves $(M = 2)$ is analysed here to validate the fundamental performance of the proposed algorithm. In this case, the eigenvalues are given as follows [13]

$$\lambda_1 = P_n + \frac{1}{2}\left\{\xi_1 + \xi_2 + \sqrt{(\xi_1 - \xi_2)^2 + 4\xi_1\xi_2\xi_3}\right\} \tag{14}$$

$$\lambda_2 = P_n + \frac{1}{2}\left\{\xi_1 + \xi_2 - \sqrt{(\xi_1 - \xi_2)^2 + 4\xi_1\xi_2\xi_3}\right\} \tag{15}$$

$$\lambda_i = P_n \quad (i = 3, \ldots, K) \tag{16}$$

where

$$\xi_1 = P_d\tilde{D}(\phi_d) \quad (\xi_1 > 0) \tag{17}$$

$$\xi_2 = P_u\tilde{D}(\phi_u) \quad (\xi_2 > 0) \tag{18}$$

$$\xi_3 = |\rho|^2 \quad (0 \leq \xi_3 \leq 1) \tag{19}$$

ξ_1 and ξ_2 express the summations of input powers received at each of the elements for a desired wave and an interference wave, respectively. Substituting (14) and (15) into (8)–(10), the objective functions are represented by

$$J_1 = P_n + \frac{1}{2}\left\{\xi_1 + \xi_2 - \sqrt{(\xi_1 - \xi_2)^2 + 4\xi_1\xi_2\xi_3}\right\} \tag{20}$$

$$J_2 = \xi_1\xi_2(1 - \xi_3) + P_n(\xi_1 + \xi_2) + P_n^2 \tag{21}$$

$$J_3 = \frac{\xi_1\xi_2}{\xi_1 + \xi_2 + 2P_n}(1 - \xi_3) + P_n - \frac{P_n^2}{\xi_1 + \xi_2 + 2P_n} \tag{22}$$

Assuming that J_i $(i = 1, 2, 3)$ are the continuous functions of ξ_i $(i = 1, 2, 3)$, the following relations can be obtained

$$\frac{\partial J_1}{\partial \xi_1}, \frac{\partial J_1}{\partial \xi_2} \geq 0 \tag{23}$$

$$\frac{\partial J_2}{\partial \xi_1}, \frac{\partial J_2}{\partial \xi_2} > 0 \tag{24}$$

$$\frac{\partial J_3}{\partial \xi_1}, \frac{\partial J_3}{\partial \xi_2} > 0 \tag{25}$$

$$\frac{\partial J_1}{\partial \xi_3}, \frac{\partial J_2}{\partial \xi_3}, \frac{\partial J_3}{\partial \xi_3} < 0 \tag{26}$$

where we have equality if and only if $\xi_3 = 0$. The derivations of (23)–(26) are provided in the appendix. Equations (23)–(26) mean that maximising one of the proposed objective functions implicitly promotes both the increase in $\tilde{D}(\phi_d)$, $\tilde{D}(\phi_u)$ and the reduction in $|\rho|$.

It should be noted that there is no restriction in sampling points of $\boldsymbol{s}$. Thus, multiple snap shots can be gathered while receiving one symbol. In this point, the algorithm is similar to the constant modulus algorithm, which is atypical example of a blind algrithm.

The proposed system has the different missions with respect to each of the two-stage controls, that is, pattern optimisation and interference cancellation. As already noted, the goal at the first stage is to maximise the received powers in the signal subspace regardless of the desired wave or the interference wave, and to reduce the spatial correlation coefficient between incident waves, which enhances the performance of the next stage. Notice that null forming towards the interference wave is not the

doi: 10.1049/iet-map:20070076

objective at this stage. At the second stage, the separation of the waves is conducted to obtain high array output SINR.

3 Performance analysis and discussion

3.1 Computer simulation

In order to verify the effects of the proposed algorithm, computer simulation is carried out on a K-element linear array with spacing of λ. For simplicity, we assume two uncorrelated waves, that is, a desired wave and an interference wave, are incident throughout the simulation. An electronically steerable parasitic array radiator (ESPAR) antenna is adopted as each antenna element of the hybrid smart antenna system [7]. The configuration and specifications of the ESPAR antenna used in the simulation are shown in Fig. 2 and Table 1, respectively. The pattern of the ESPAR antenna is formulated as a continuous function of the L variable reactance circuits embedded in the ESPAR antenna. Consequently, the element patterns in this system are represented by

$$f_j(\phi) = f_j(\boldsymbol{x}_j, \phi) \quad (j = 1, \ldots, K) \tag{27}$$

where

$$\boldsymbol{x}_j = [x_{j1} x_{j2} \cdots x_{jL}]^{\mathrm{T}} \tag{28}$$

and x_{jl} represents a reactance value of the lth reactance circuit ($l = 1, 2, \ldots, L$) in the jth element. For simplicity, the impedance and polarisation of each of the ESPAR antenna units are assumed to be matched, and mutual coupling between any two ESPAR antenna units is ignored.

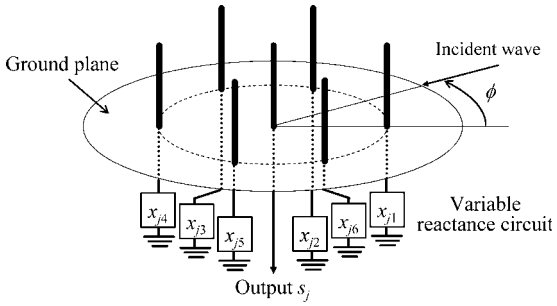

Figure 2 *Configuration of ESPAR antenna used in computer simulation as jth element of hybrid smart antenna ($L = 6$)*

Table 1 Specifications of ESPAR antenna

number of reactance circuits L	6
spacing between an active element and parasitic elements	$\lambda/4$
range of reactance values x_l [Ω] ($l = 1, 2, \ldots, L$)	$-100 < x_l < 100$
operating frequency	2.4 GHz

To maximise one of the proposed objective functions J_i ($i = 1, 2, 3$), the steepest descent method [9] is used in this simulation

$$\boldsymbol{x}_j(m+1) = \boldsymbol{x}_j(m) + \mu \frac{\nabla_j J_i}{|\nabla_j J_i|} \quad (j = 1, \ldots, K) \tag{29}$$

where ∇_j is the gradient operator expressed by

$$\nabla_j = \left[\frac{\partial}{\partial x_{j1}} \frac{\partial}{\partial x_{j2}} \cdots \frac{\partial}{\partial x_{jL}} \right]^{\mathrm{T}} \tag{30}$$

and μ is the step width. Here, the derivative operation is calculated as the difference operation in the computer simulation. Note that the perturbations have to be implemented with all of the reactance circuits of K ESPAR antennas unlike only one ESPAR antenna control in [9]. The solving method in (31) does not guarantee a global optimum solution, and its solution is greatly influenced by the initial values and the variable ranges of the reactance circuits, which is similar to [9]. Additionally, it is obvious that the calculation of J_1, J_2 or J_3 is not so complex because the order of the covariance matrix is two. To show the improvement of the hybrid smart antenna system, we consider the DBF antenna array using omni-directional elements as a conventional system. The configuration of the conventional system is the same as the hybrid smart antenna system except for the elements. Here, each element gain is given by 3 dBi, which is nearly equal to the gain of the ESPAR antenna with the reactance values of zeros. The simulation conditions are described in Table 2. Also, the input SNR and INR are equal to 30 dB unless otherwise noted.

First, it is assumed that $\phi_d = 0^\circ$ and $\phi_u = 105^\circ$ in the simulation shown in Figs. 3–6. This condition gives

Table 2 Simulation conditions

Smart antenna system and environment	
proposed system configuration	uniform linear array of ESPAR antennas
conventional system configuration	uniform linear array of omni-directional antennas (3 dBi)
element spacing	λ
number of elements	2
number of waves	2
Eigenspace control algorithm	
Step width μ for steepest descent method	3
Number of snap shot	100
Initial reactance values $\boldsymbol{x}_1$, $\boldsymbol{x}_2$	$\mathbf{0} = [0\ 0\ 0\ 0\ 0\ 0]^{\mathrm{T}}$

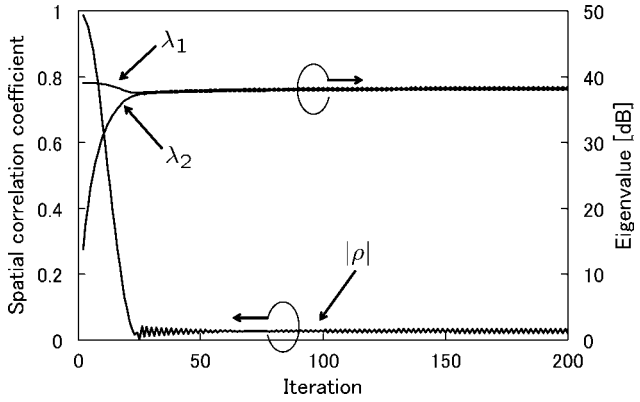

Figure 3 *Convergence of spatial correlation coefficient and eigenvalues in the proposed algorithm using J_1, where each eigenvalue is normalised by P_n ($\phi_d = 0^\circ$, $\phi_u = 105^\circ$, and SNR = INR = 30 dB)*

$|\rho| = 0.99$ in the conventional system, which is a grating relation between incident waves. This case is chosen to clarify that the proposed algorithm can overcome such a severe condition, that is to say, much high $|\rho|$. Fig. 3 shows the convergence characteristics of λ_1, λ_2 and $|\rho|$ in the proposed algorithm using J_1, where λ_1 and λ_2 are normalised by P_n. The initial values of $\boldsymbol{x}_1$, $\boldsymbol{x}_2$ are given by zeros. As shown in Fig. 3, the proposed algorithm drastically reduces the $|\rho|$ and increases λ_2 with increase of the iteration number.

Fig. 4 shows the convergence characteristics of array output SINR controlled using least mean squares (LMS) and recursive least squares (RLS) after the proposed control of the elements. For simplicity, it is assumed that the exact reference signal is obtained in the system by some means. The LMS and RLS are based on sampling feedback control with the algorithms shown in [14, 15]. Here, the step width for LMS and the forgetting factor for RLS are 0.02 and 0.9, respectively. As shown in Fig. 4, the proposed system achieves much faster convergence than the conventional system when using LMS, because the

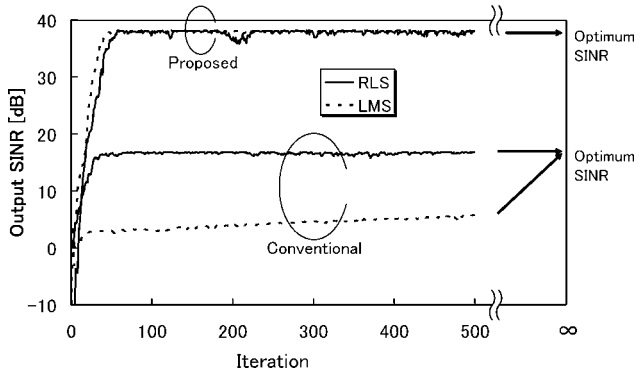

Figure 4 *Convergence of output SINR for hybrid smart antenna system and conventional system using LMS algorithm and RLS algorithm for complex weights ($\phi_d = 0^\circ$, $\phi_c = 105^\circ$, and SNR = INR = 30 dB)*

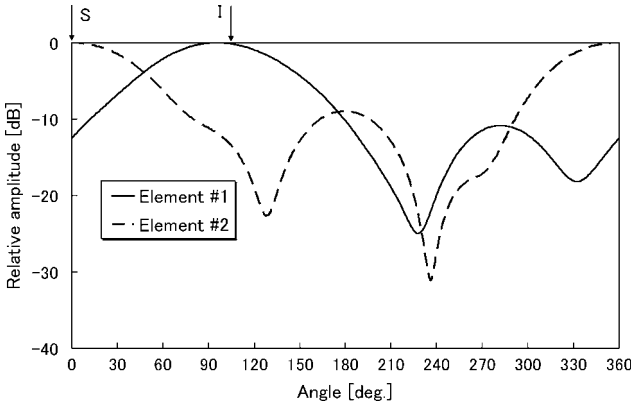

Figure 5 *Radiation patterns of hybrid smart antenna elements controlled by the proposed algorithm using J_1 ($\phi_d = 0^\circ$, $\phi_u = 105^\circ$, and SNR = INR = 30 dB)*

problem of the eigenvalue spread of covariance matrix is improved by the reduction of $|\rho|$ [13, 15]. Also, the LMS shows nearly the same convergence as RLS in the proposed system. It is found that both high convergence rate and reduction of computational load can be attained by LMS with the proposed algorithm.

Fig. 5 shows each of the patterns determined by the proposed algorithm. It is observed that each of the elements has a radiation pattern with the main lobe towards either of the waves. Each of the elements does not create any deep nulls towards the incident waves, which is consistent with the concept on the first-stage control. Fig. 6 shows the array output pattern of the hybrid smart antenna system using optimum weights $\boldsymbol{w}_{\text{opt}}$, which is given as follows

$$\boldsymbol{w}_{\text{opt}} = R^{-1}\boldsymbol{v}(\phi_d) \tag{31}$$

where $\boldsymbol{w}_{\text{opt}}$ gives the optimum SINR as shown in Fig. 4. In the proposed algorithm, high SINR is attained by forming a

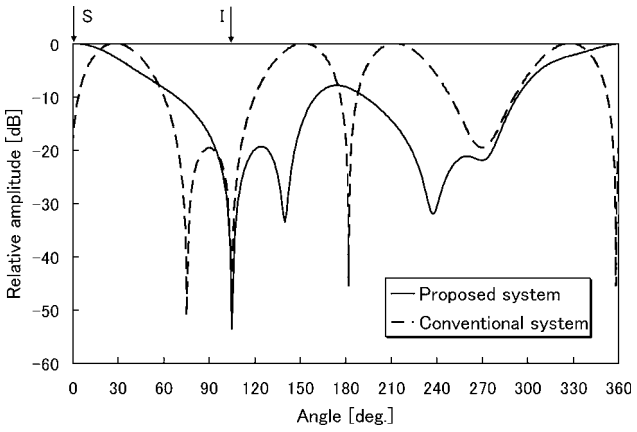

Figure 6 *Comparison between hybrid smart antenna system and conventional system of array output patterns using optimum weights ($\phi_d = 0^\circ$, $\phi_u = 105^\circ$, and SNR = INR = 30 dB)*

doi: 10.1049/iet-map:20070076

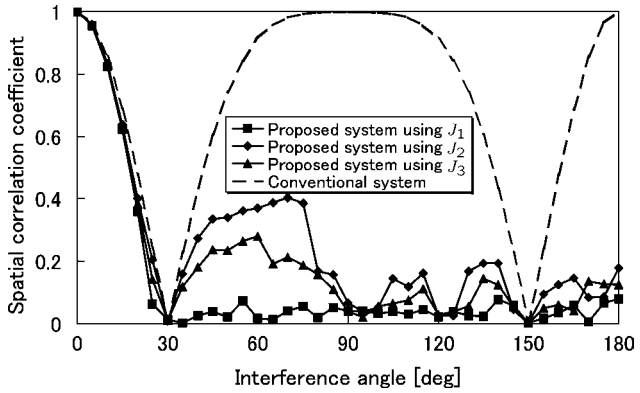

Figure 7 *Comparison of spatial correlation coefficients in hybrid smart antenna system among the proposed objective functions for $\phi_d = 0$, SNR = INR = 30 dB*

null towards the interference wave effectively while receiving the desired wave. On the other hand, the conventional system formed the null towards not only the interference wave but also the desired wave, which is called a grating null.

To show the influence of DOA on the reduction of $|\rho|$ obtained from the result of the proposed algorithm, the relations between $|\rho|$ and ϕ_u with $\phi_d = 0^\circ$ fixed are shown in Fig. 7. It is found that all of the proposed objective functions show much lower $|\rho|$ than the conventional system outside the range $|\phi_u| \leq 30^\circ$. This range depends on the system configuration, especially on the element spacing and the beamwidth of each element. Also, the performance by J_1 represents the lowest $|\rho|$ of the proposed objective functions.

Next, the statistical performance is examined in terms of a cumulative distribution function (CDF) of array output SINR by optimum weight given by (31). We simulate 1000 random DOA cases of the two waves for each array output SINR. Fig. 8 shows the CDF of array output SINR for the hybrid smart antenna using each of the objective functions. There is little difference in the performance

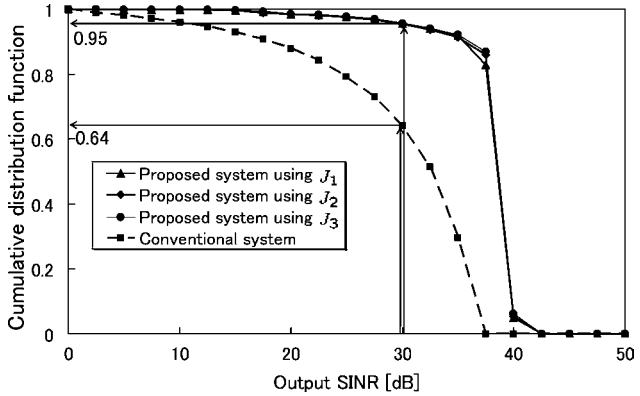

Figure 8 *Comparison of CDFs of output SINR in hybrid smart antenna system among the proposed objective functions for SNR = INR = 30 dB*

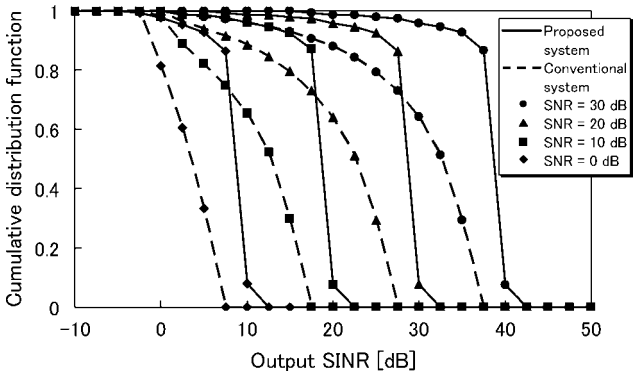

Figure 9 *Comparison of CDFs of output SINR between hybrid smart antenna system using J_1 and conventional system for SNR = 0, 10, 20 and 30 dB*

among the proposed objective functions. This is because the array output SINR in (4) includes $|\rho|^2$ and is insensitive to $|\rho|$ if $|\rho|$ can be reduced to some extent in the algorithm. In each of the proposed systems, more than 95% of the array output SINR exceeds 30 dB, which is equal to input SNR or INR. In the conventional system, on the other hand, the percentage of the array output SINR exceeding 30 dB is $<65\%$. It is clear that the proposed systems realise more stable and higher performance than the conventional system.

Fig. 9 shows the dependence of the CDFs on P_n in the hybrid smart antenna system using J_1. We change the input SNR from 0 to 30 dB by 10 dB with input INR kept equal to the input SNR. Regardless of the input SNR, the CDFs in the proposed system show similar characteristics. In fact, $>95\%$ of the array output SINR in the proposed system exceeds a value equal to the input SNR. Consequently, the proposed algorithm using J_1 is found to be robust to the thermal noise.

To quantitatively compare the effect of ρ with that of element gains on the performance of the hybrid smart antenna system, we introduce the virtual values of SINR represented as follows

$$\mathrm{SINR}_{\rho} = \frac{KP_d}{P_n}\left(1 - \frac{KP_u}{P_n + KP_u}|\rho|^2\right) \tag{32}$$

$$\mathrm{SINR}_{\tilde{D}} = \frac{P_d\tilde{D}(\phi_d)}{P_n}\left(1 - \frac{P_u\tilde{D}(\phi_u)}{P_n + P_u\tilde{D}(\phi_u)}|\rho_0|^2\right) \tag{33}$$

where ρ_0 is the spatial correlation coefficient of the conventional system. Equation (32) represents the virtual SINR characterised by only the improvement of ρ, which is obtained by substituting K into $\tilde{D}(\phi_d)$ and $\tilde{D}(\phi_u)$ in (4). In a similar way, (33) represents the virtual SINR characterised by only the improvement of element gains, which is obtained by substituting ρ_0 into ρ_0 in (4). Fig. 10 shows the CDFs of output SINR of (4), (32) and (33) in the hybrid smart antenna system using J_1. From the CDF

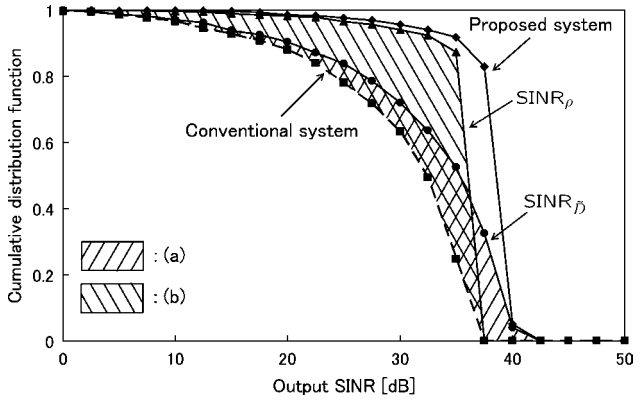

Figure 10 *Effects of spatial correlation coefficient and element gains on performance of hybrid smart antenna system using J_1*

of (33), the element gains contribute to improvement in the wide range of SINR over the conventional system because of the increase of received powers, which is represented by the shaded area in Fig. 10*a*. On the other hand, the CDF of (32) shows the drastic improvement especially in the range of low SINR, represented by the shaded area in Fig. 10*b*. It is clear that the effect of the latter is more dominant than the former. From the point of view of low SINR compensation, each element does not need high gain if $|\rho|$ can be reduced effectively. It should also be noted that all the reactance circuits converged stably as far as the computations were carried out in this paper.

The simulations were carried out for the case of two incident waves, but the proposed algorithm can be applied for the case of more than two incident waves as far as the number of incident waves are less than the number of steerable antennas. On the other hand, all of the interferences cannot be suppressed when the number of steerable antennas is less than the number of incident waves. This limitation is the same as that in conventioanl adaptive arrays. However, such severe situations can be avoided by an appropriate medium access control (MAC) design. Additionally, it should be noted that SDMA is compatible with other multiple access schemes such as TDMA, FDMA and CDMA. Their capacities are multiplied by the capacity of the SDMA in the combination. Therefore it can be said that the proposed algorithm is useful even in the case that the capacity of SDMA is low.

Although the cases with uncorrelated waves have been discussed above, the increase of the number of waves may be because of multipath. Generally, the waves induced from the same signal source are correlated, and do not change the configuration of the eigenvalues which are calculated from covariance matrix at the proposed receiver. Therefore it can be anticipated in this case that the proposed eigenvalue-based algorithm optimises each steerable antenna so as to reduce the correlation between uncorrelated signal sources. After the optimisation of the steerable antennas, DBF can be successfully implemented.

3.2 Modification of the proposed objective functions

Furthermore, the proposed objective functions shown in (9) and (10) are modified to reduce the computational load. The modified functions can be expressed as follows

$$J_2' = \lambda_1 \cdots \lambda_K = \det(R) \tag{34}$$

$$J_3' = \frac{\lambda_1 \cdots \lambda_K}{\lambda_1 + \cdots + \lambda_K} = \frac{\det(R)}{\mathrm{tr}(R)} \tag{35}$$

where the det and tr operations denote the determinant and summation of diagonal components, respectively. These modified objective functions J_2' and J_3' have the advantage of being calculated not by solving the eigenvalue problem but by the det and/or tr operations. When $K = M$, (34) and (35) are mathematically equal to (9) and (10), respectively. Otherwise, the difference between (35) and (9) is only the fixed bias V which is given by

$$V = \lambda_{M+1} \cdots \lambda_K = P_n^{K-M} \tag{36}$$

Consequently, they show the same characteristics in essence. These modifications are effective especially for the case of many elements, because the computational load for solving eigenvalue problems increases in accordance with the number of elements.

3.3 Discussion

In the simulation, elements with continuously controllable patterns were adopted, and the proposed algorithm was implemented using the steepest descent method. It is clear that the elements and/or the solution of the algorithm can be replaced by the other ones. For example, the algorithm can be applied to the elements, some of whose patterns are prepared in advance. In this case, the proposed algorithm would be implemented by trying all of the pattern combinations. Therefore it is possible to reduce the system size, computational load and number of iterations at the cost of some degradation of performance. Also, each of the elements may be composed of switched-beam antenna, resulting in lower cost than reactively steered antenna. It is also possible to adopt DBF antenna arrays as elements with demandingly higher quality than in the simulated system, in which conventional full DBF antenna arrays can be applied to the proposed algorithm.

In terms of exploiting antenna-specific channel impulse responses of array elements, spatial division multiplexing (SDM) in multiple-input multiple-output systems is similar to SDMA [16]. This indicates the possibility that the algorithm proposed for SDMA in this paper is also applicable to SDM. This application is being studied at the moment, and will be submitted to another paper.

doi: 10.1049/iet-map:20070076

4 Conclusion

In this paper, we have proposed a novel algorithm and concept for a hybrid smart antenna system. Unlike traditional examples, this algorithm controls the directional elements on the basis of a proposed objective function, which is composed of eigenvalues of a covariance matrix. The algorithm provides a high array output SINR both an increase in the received powers and a reduction in the spatial correlation coefficient of incident waves. As these characteristics are realised in an implicit manner, the algorithm does not require prior knowledge of DOA, CSI or training signals. To verify the effect of the proposed algorithms, both a theoretical and numerical approach were taken with a case of two incident waves. Theoretically, the algorithm was proved to reduce $|\rho|$ and to increase input power depending on DOA. From the simulation, convergence using an LMS algorithm was shown to be as fast as an RLS algorithm because of the improvement in the eigenvalue spread of the covariance matrix. Next, the algorithm was found to be robust to thermal noise. Then, through a statistical performance evaluation, it was confirmed that the reduction of $|\rho|$ has a more dominant effect than the increase of element gains on the improvement of output SINR. Additionally, we have shown a method to realise the proposed algorithm using the objective functions J_2 or J_3 without solving the eigenvalue problem. Analysis of the proposed algorithm for cases with more incident waves is an important further study for practical designs.

In the future, the proposed algorithm will be useful especially in smart antenna system applications required for the reduction of spatial correlation between incident waves.

5 References

[1] CHRYSSOMALLIS M.: 'Smart antennas', *IEEE Antennas Propag. Mag.*, 2000, **42**, (3), pp. 129–136

[2] HAYKIN S.: 'Adaptive filter theory' (Prentice Hall, 1991, 2nd edn.)

[3] KUGA N., ARAI H.: 'A flat four-beam switched array antenna', *IEEE Trans. Antennas Propag.*, 1996, **44**, (9), pp. 1227–1230

[4] NGAMJANYAPORN P., PHONGCHAROENPANICH C., AKKARAEKTHALIN P., KRAIRIKSH M.: 'Signal-to-interference ratio improvement by using a phased array antenna of switched-beam elements', *IEEE Trans. Antennas Propag.*, 2005, **53**, (5), pp. 1819–1828

[5] HARRINGTON R.F.: 'Reactively controlled directive arrays', *IEEE Trans. Antennas Propag.*, 1978, **26**, (3), pp. 390–395

[6] DINGER R.J.: 'A planar version of a 4.0 GHz reactively steered adaptive array', *IEEE Trans. Antennas Propag.*, 1986, **34**, (3), pp. 427–431

[7] SCHLUB R., LU J., OHIRA T.: 'Seven element ground skirt monopole ESPAR antenna design from a genetic algorithm and the finite element method', *IEEE Trans. Antennas Propag.*, 2003, **51**, (11), pp. 3033–3039

[8] CHENG J., KAMIYA Y., OHIRA T.: 'Adaptive beamforming of ESPAR antenna using sequential perturbation'. Proc. IEEE MTT-S Int. Microwave Symp. Digest, 2001, vol. 1, pp. 133–136

[9] SUN C., HIRATA A., OHIRA T., KARMARKAR N.C.: 'Fast beamforming of electronically steerable parasitic array radiator antennas: theory and experiment', *IEEE Trans. Antennas Propag.*, 2004, **52**, (7), pp. 1819–1832

[10] WIN M.Z., BEAULIEU N.C., SHEPP L.A., LOGAN B.F.JR., WINTERS J.H.: 'On the SNR penalty of MPSK with hybrid selection/maximal ratio combining over i.i.d. Rayleigh fading channels', *IEEE Trans. Commun.*, 2003, **51**, (6), pp. 1012–1023

[11] ZHANG Z., ISKANDER M.F., YUN Z., MADSEN A.H.: 'Hybrid smart antenna system using directional elements-performance analysis in flat Rayleigh fading', *IEEE Trans. Antennas Propag.*, 2003, **51**, (10), pp. 2926–2935

[12] REZK M., KIM W., YUN Z., ISKANDER M.F.: 'Performance comparison of a novel hybrid smart antenna system versus the fully adaptive and switched beam antenna arrays', *IEEE Antennas Wirel Propag. Lett.*, 2005, **4**, pp. 285–288

[13] LIN H.-C.: 'Spatial correlation in adaptive arrays', *IEEE Trans. Antennas Propag.*, 1982, **30**, (2), pp. 212–223

[14] WIDROW B., STEARNS S.D.: 'Adaptive signal processing' (Prentice Hall, 1985)

[15] COMPTON R.T. JR.: 'Adaptive antennas – concepts and performance' (Prentice Hall, 1988)

[16] JIANG M., HANZO L.: 'Multiuser MIMO–OFDM for next generation wireless systems', *Proc. IEEE*, 2007, **95**, (7), pp. 1430–1469

6 Appendix: mathematical inequalities

Derivation of mathematical inequalities (23)–(26) is carried out in this appendix. First, the total differentiation of the proposed objective functions are expressed by

$$\mathrm{d}J_i = \alpha_i\,\mathrm{d}\xi_1 + \beta_i\,\mathrm{d}\xi_2 + \gamma_i\,\mathrm{d}\xi_3 \quad (i = 1, 2, 3) \qquad (37)$$

where

$$\alpha_i = \frac{\partial J_i}{\partial \xi_1} \tag{38}$$

$$\beta_i = \frac{\partial J_i}{\partial \xi_2} \tag{39}$$

$$\gamma_i = \frac{\partial J_i}{\partial \xi_3} \tag{40}$$

By using (20)–(22) and (38)–(40), (37) are rewritten by

$$\begin{aligned} \mathrm{d}J_1 = {} & \frac{1}{2}\left\{1 - \frac{\xi_1 - \xi_2 + 2\xi_2\xi_3}{\sqrt{(\xi_1 - \xi_2)^2 + 4\xi_1\xi_2\xi_3}}\right\}\mathrm{d}\xi_1 \\ & + \frac{1}{2}\left\{1 - \frac{\xi_2 - \xi_1 + 2\xi_1\xi_3}{\sqrt{(\xi_1 - \xi_2)^2 + 4\xi_1\xi_2\xi_3}}\right\}\mathrm{d}\xi_2 \\ & - \frac{\xi_1\xi_2}{\sqrt{(\xi_1 - \xi_2)^2 + 4\xi_1\xi_2\xi_3}}\mathrm{d}\xi_3 \end{aligned} \tag{41}$$

$$\begin{aligned} \mathrm{d}J_2 = {} & \{\xi_2(1 - \xi_3) + P_n\}\mathrm{d}\xi_1 \\ & + \{\xi_1(1 - \xi_3) + P_n\}\mathrm{d}\xi_2 - \xi_1\xi_2\,\mathrm{d}\xi_3 \end{aligned} \tag{42}$$

$$\begin{aligned} \mathrm{d}J_3 = {} & \frac{\xi_2(1 - \xi_3)(\xi_2 + 2P_n) + P_n^2}{(\xi_1 + \xi_2 + 2P_n)^2}\mathrm{d}\xi_1 \\ & + \frac{\xi_1(1 - \xi_3)(\xi_1 + 2P_n) + P_n^2}{(\xi_1 + \xi_2 + 2P_n)^2}\mathrm{d}\xi_2 \\ & - \frac{\xi_1\xi_2}{\xi_1 + \xi_2 + 2P_n}\mathrm{d}\xi_3 \end{aligned} \tag{43}$$

Consequently, the results as shown below can be obtained

$$\alpha_2, \beta_2 > 0 \tag{44}$$

$$\alpha_3, \beta_3 > 0 \tag{45}$$

$$\gamma_j < 0 \quad (j = 1, 2, 3) \tag{46}$$

Finally, (23) is derived as follows

$$\begin{aligned} & \left(\sqrt{(\xi_1 - \xi_2)^2 + 4\xi_1\xi_2\xi_3}\right)^2 - (\xi_1 - \xi_2 + 2\xi_2\xi_3)^2 \\ & = 4\xi_2^2\xi_3(1 - \xi_3) \geq 0 \end{aligned} \tag{47}$$

$$\Longleftrightarrow \left|\frac{\xi_1 - \xi_2 + 2\xi_2\xi_3}{\sqrt{(\xi_1 - \xi_2)^2 + 4\xi_1\xi_2\xi_3}}\right| \leq 1 \tag{48}$$

Therefore

$$\alpha_1 = \frac{1}{2}\left\{1 - \frac{\xi_1 - \xi_2 + 2\xi_2\xi_3}{\sqrt{(\xi_1 - \xi_2)^2 + 4\xi_1\xi_2\xi_3}}\right\} \geq 0 \tag{49}$$

In the same way

$$\alpha_2 = \frac{1}{2}\left\{1 - \frac{\xi_1 - \xi_2 + 2\xi_1\xi_3}{\sqrt{(\xi_1 - \xi_2)^2 + 4\xi_1\xi_2\xi_3}}\right\} \geq 0 \tag{50}$$

where we have equality if and only if $\xi_3 = 0$ in (49) and (50).

doi: 10.1049/iet-map:20070076